Paper

Magnetic and magneto-dielectric properties of magneto-electric field effect capacitor using Cr_2O_3

Takeshi YOKOTA,[†] **Shotaro MURATA, Takaaki KURIBAYASHI and Manabu GOMI**

Materials Science and Engineering, Nagoya Institute of Technology, Gokiso-cho, Showa-ku, Nagoya, Aichi, 466−8555

We investigated the magnetic and dielectric properties of a metal (Pt)/insulator (Cr_2O_3)/magnetic floating gate (Fe)/tunnel layer (CeO_2)/semiconductor (Si) capacitor. This capacitor shows capacitance–voltage (*C–V*) properties typical of a Si Metal-Insulator-Semiconductor (MIS) capacitor with hysteresis, which indicates that electrons have been injected into the Fe layer. The capacitor also shows ferromagnetic properties. The *C–V* curve has a hysteresis window with a clockwise trace. This hysteresis behavior was changed by the application of an external magnetic field. These results indicate that this MIS capacitor contains a ferromagnetic floating gate and a magneto-electric insulating layer in a single system.
©2008 The Ceramic Society of Japan. All rights reserved.

1. Introduction

Magneto-electronics employing magneto-electric (ME) materials have become attractive as new generation non-volatile data storage devices because their magnetic or ferroelectric properties can be controlled by an external electric or magnetic field. For example, reports have described cross-coupling involving polarization reversal through the application of a magnetic field to $TbMn_2O_5$ and the electric field-stimulated ferromagnetic order in hexagonal $HoMnO_3$.[1),2)] Epitaxially grown $BiFeO_3$ films have shown an enhancement of ferroelectric polarization and related properties by more than an order of magnitude in comparison to bulk $BiFeO_3$.[3),4)] However, most of those materials have a relatively low magnetic Curie temperature, i.e., less than 270 K.

The present study focused on the ME material Cr_2O_3 in spintronics applications. The Néel temperature of Cr_2O_3 is 307 K and the ME effect is expected to occur at room temperature. However, the magnetic moment induced by an electric field of 10^5 Vm^{-1} is only 10^{-5} μ_B per Cr atom.[5)–7)] In order to make efficient use of the magnetic moment, we propose the use of Cr_2O_3 film as a control gate insulator of a MIS capacitor which includes a magnetic floating gate (MFG). Use of the induced magnetic moment might provide a sufficiently high degree of control of the other magnetic spin states, especially very tiny spin. Hence, we predict that the induced magnetic moment will affect electromagnetically the stored charge state in an ultra-thin MFG layer. To achieve this purpose, in the present paper we prepared magneto-electric field effect capacitors (MECs) and investigated the magnetic and dielectric properties.

2. Experiment

MECs were prepared using the 3-guns radio-frequency magnetron sputtering method. Cr_2O_3 and CeO_2 sintered ceramics were used as the target. The base pressure before introducing the sputtering gas was 3.0×10^{-4} Pa and the gas pressure during deposition was 8.0×10^{-1} Pa. The first CeO_2 tunnel layer was

deposited on an n-type Si (111) substrate cleaned using improved Radio Corporation America methods. The thickness of the first layer was changed from 5 to 15 nm. MFG, which is a Fe layer with a thickness of 1.5 nm, was then deposited using only Ar as the sputtering gas. Finally, a Cr_2O_3 layer of 45 nm was deposited. The magnetic properties of the sample were measured using a Superconducting Quantum Interface Device. The structural analysis of the films was performed using an X-ray diffractometer (XRD) utilizing Cu Kα radiation and Reflected High Energy Electron Diffraction (RHEED). The surface morphology was measured using an Atomic Force Microscope (AFM). The leakage current was measured using a picoammeter (Keithley-6487), while capacitance was measured using a LCR meter (Wayne Kerr 6440A). Pt and Au were used as a top and bottom electrode, respectively. To avoid a measurement deviation, electric property measurements were performed using about 40 electrodes constructed on the sample. A schematic illustration is shown in Fig. 2.

3. Results and discussion

It is well known that oxide films are difficult to be directly deposit on Si without any SiO_x in the interface. In order to prevent this problem, CeO_2 was used as a first tunnel layer, because the Gibbs Free Energy of CeO_2 is higher than that of SiO_x. Moreover, the lattices mismatch between the CeO_2 (111) and Si (111) substrate is about 0.35%. This means that the CeO_2 can be directly grown on Si substrate.[8),9)] Since no crystallographic differences such as d-spacing changes, intensity changes and full width at half maximum are observed by changing the thicknesses of the CeO_2 and MFG layers, respectively, typical XRD and RHEED patterns of the Cr_2O_3/MFG/CeO_2/Si capacitor were produced, as shown in **Fig. 1**. Cr_2O_3 polycrystalline diffraction and highly oriented CeO_2 diffraction patterns were observed. This result supported our expectation mentioned above. According to an analysis of the RHEED pattern, Cr_2O_3 film has preferentially 006-oriented structures. **Figure 2** shows the CeO_2 tunnel layer's dependence on the thickness of the (a) *I–V* and (b) *C–V* characteristics of the sample. The inset shows a schematic illustration of the measurement. The leakage current density decreased with

† Corresponding author: T. Yokota; E-mail: yokota.takeshi@nitech. ac.jp

the increases in the thickness of the tunnel layer. Although thick insulator produces high resistivity, the leakage current density of the sample having a 15 nm tunnel layer was high. The *C–V* curves show hysteresis due to insertion of the MFG layers. The curve of the sample having a 15 nm tunnel layer has hysteresis showing a counterclockwise trace, which indicates that the film has mobile ionic charges. The other films having other tunnel layer thicknesses show a clockwise trace, which indicates that electrons have been injected into the ultra-thin Fe layer. Although the sample having a 10 nm tunnel layer showed the lowest leakage current, the hysteresis window width decreased compared with the sample having a 5 nm tunnel layer. In order to investigate the *I–V* and *C–V* curves differences among samples, surface morphology of CeO_2 layers were measured using AFM. The AFM images were measured using a 1 nm lift height. **Figure 3** shows AFM images and the line profiles, which is corresponding to the white line on the images, of the surface of CeO_2 film with various thicknesses. According to the line profiles, the surface morphology of the sample with the thickness of 10 nm is the smoothest among the samples. On the other hand, 15 nm sample's surface is obviously rough. This is probably due

to the crystal growth mode of CeO_2 film at high temperatures. Below 10 nm thickness, CeO_2 film seems to be 2-dimentionally grown until CeO_2 film was fully covered Si surface. And then film was 3-dimentionally grown. With the increases of the CeO_2 thickness, stress of CeO_2 film due to the lattice mismatch was
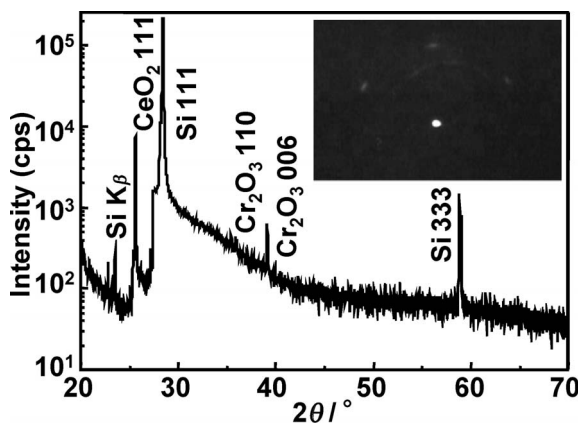

Fig. 2. (a) *I–V* and (b) *C–V* characteristics of the Cr_2O_3/Fe/CeO_2/Si capacitor with various CeO_2 thicknesses.

Fig. 1. XRD and RHEED patterns of Cr_2O_3(45 nm)/Fe(1.5 nm)/ CeO_2(5 nm)/Si capacitor.
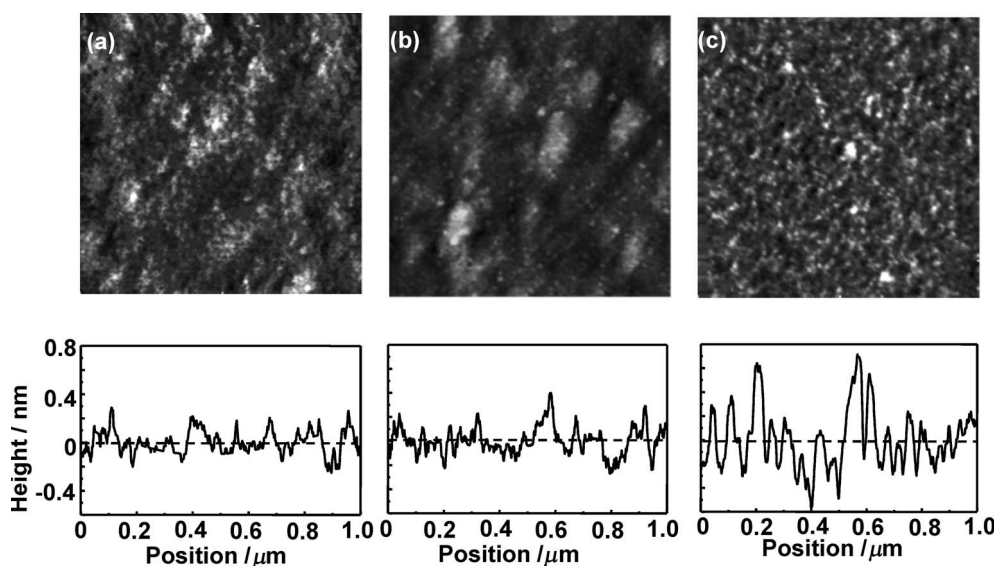

Fig. 3. AFM images and line profiles of CeO_2 films with the thickness of (a) 5 nm, (b) 10 nm, (c) 15 nm. The AFM images were measured using a 1 nm lift height and Line profiles were measured along cursor indicated on AFM images.

relaxed. Consequently, CeO_2 film was 3-dimentionally grown with the arrangement of CeO_2, making CeO_2 (111) in-plane random.[8] This makes highly oriented CeO_2 film shows a columnar structure with an increase in thickness. The leakage current density differences among samples can be explained by these surface morphology differences. Since the samples have smooth surface below a thickness of 10 nm, the leakage current decreases with the increases of CeO_2 thickness. However, the sample with the thickness of 15 nm has rough surface with a columnar structure, which causes high leakage current along the crystal grain boundary. The $C–V$ curves also were explained by the $I–V$ properties. The sample having a 10 nm tunnel layer is too thick to allow the tunneling effect, and thus a sufficient electron charge cannot be injected into the MFG layer from Si. On the other hand, the sample having a 15 nm tunnel layer has rough surface roughness. When the Fe was deposited on this rough surface, the mobile ionic charge or space charge, which gives rise to the high leakage current density, could be generated between Fe and CeO_2. Therefore, the $C–V$ curves showed the hysteresis a counterclockwise trace.

Since a sample expressing the memory effect using ME material was prepared, its magnetic properties were also measured. **Figure 4** shows the magnetization curve of the sample having a 5 nm tunnel layer. The saturation magnetization was about 200 emu/cc. Since there are no magnetic properties differences among samples with different CeO_2 thickness, this magnetic property is responsible for the inserted Fe layer. It seems that Fe wasn't oxidized during the deposition. It is difficult to determine the volume of the MFG layer because of its thinness. Therefore, the measurement values were divided by both the thickness of 1.5 nm and the sample area. If the Fe moment showed theoretical values of 1728 emu/cc, the coverage area of the Fe films against the surface area were about 12%. According to this estimation, Fe should exist in the form of dispersed particles because electric properties such as charge injection properties seen in the $C–V$ measurement didn't show any differences between each electrode.

In order to understand the relationships among magnetic, magneto-electric and charge injection properties, $C–V$ properties with and without an external magnetic field were measured. **Figure 5** shows the $C–V$ curves of the sample with and without the application of a magnetic field of 0.5 T. The squareness of the $C–V$ curve was enhanced by applying the magnetic field, and the capacitance values of the carrier accumulation region are
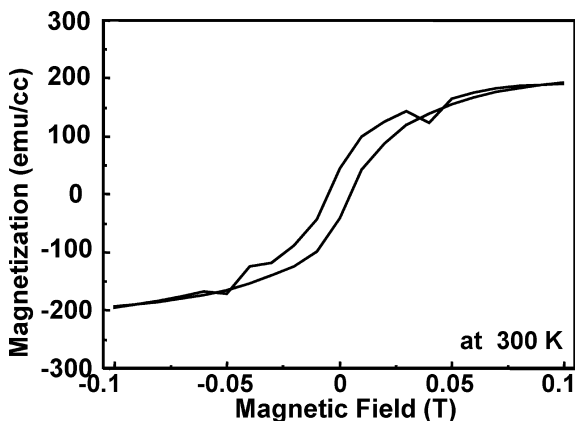
changed also by the magnetic field's application. The value of capacitance changes is up to about 20 pF. With the increases of the CeO_2 thickness, these changes become small. This behavior can be reproduced in at least 20 measurements. Although we haven't yet determined the physical origin of this behavior, one possible explanation can be proposed. Occurrence of the hysteresis window could be explained by a threshold voltage shift due to the stored charge in the floating gate. The squareness is related to the easiness of the band bending of the insulator. The Cr_2O_3 can produce an induced polarization by applying an external magnetic field due to its ME feature and can induce an apparent change of the relative permittivity of Cr_2O_3. Or, the dielectric domain of Cr_2O_3 might be aligned electro-magnetically with the existence of both an external magnetic field and electric field,
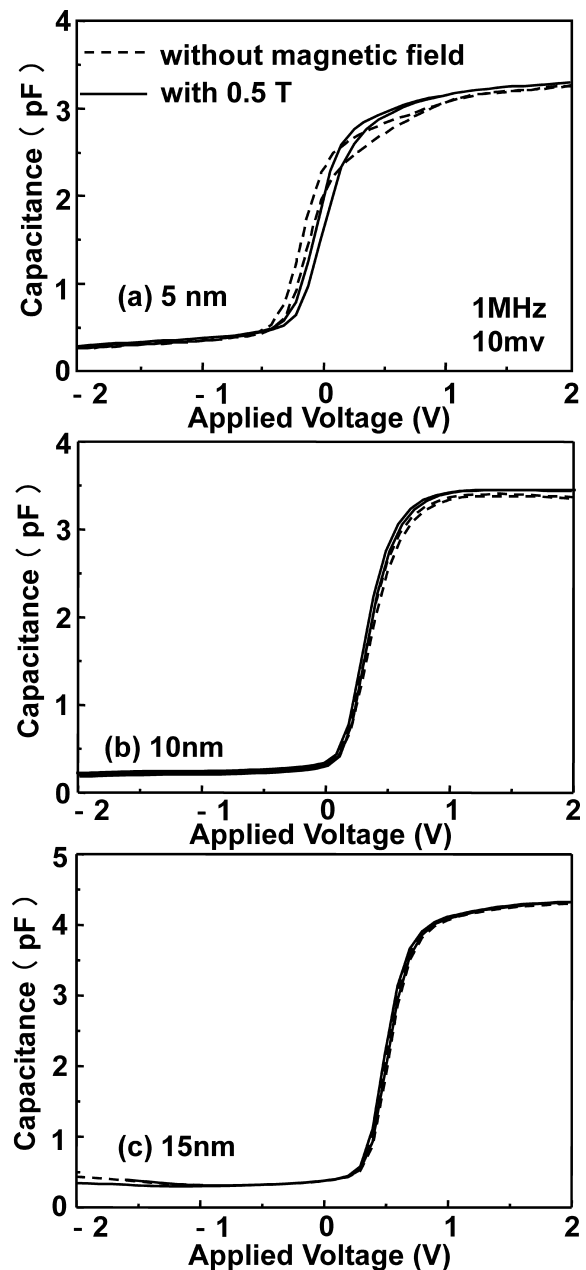

Fig. 5. $C–V$ curves of the $Cr_2O_3/Fe/CeO_2/Si$ capacitor having a (a) 5 nm (b) 10 nm (c) 15 nm CeO_2 tunnel layer with and without the application of a magnetic field of 0.5 T.

Fig. 4. Magnetization curve of Cr_2O_3(45 nm)/Fe (1.5 nm)/CeO_2(0.5 nm)/Si capacitor measured at 300 K.

which are applied for the *C–V* measurement.[10),11)] In any case, we can expect an increase in the relative permittivity of Cr_2O_3. Upon application of a voltage VG to the gate, which is top electrode on this system, an electric field is established in each of the two insulators. In other words, we have that $V_G = V_1 + V_2$ where V_1 and V_2 are the voltages developed across Cr_2O_3 and CeO_2. Therefore, increases of the relative permittivity of Cr_2O_3 give rise to an increase the voltages applied on CeO_2 layer.[12)] Band bending of CeO_2 then easily occurrs. In fact, the relative permittivity changes of the sample with 0.5 nm CeO_2 layer as estimated using the capacitance value of the accumulation region was about 0.2. This is high enough to change the applying voltage on CeO_2. On the other hand, an effective electric field applied on Cr_2O_3 film decrease with the increases of the CeO_2 thickness. The effective electric field decreases is about 30 kV/cm estimated using equivalent circuit. It could affect the magneto-electrical dielectric domain alight of Cr_2O_3. In addition, increases of CeO_2 thickness make a probability of tunneling effect reduce or generate mobile ionic charges as mentioned above. In the case of the sample with 10 nm CeO_2 film, the capacitance value was obviously changed and the squareness of the *C–V* curve is barely changed by the application of the magnetic field. Since the sample with 10 nm CeO_2 film is too thick to allow the tunneling effect, a sufficient electron charge cannot be injected into the MFG layer from Si even with the occurrence of electro-magnetical dielectric domain alignment of Cr_2O_3. In the case of the sample with 15 nm CeO_2, both the ME effect and the changes of charge injection behavior cannot be observed due to its high leakage current. Though the need more optimizing in regard to the MFG materials and the selection of tunnel layer material in order to allow their application as semiconductor memory devices, this MECs shows promise as a new spintronics device that allows inclusion of the ME effect and a charge injected memory cell in a single system. Also included in this device are typical magnetic features, such as exchange bias occurring between the ferromagnetic and antiferromagnetic materials, because the memory cell consists of both antiferromagnetic material (Cr_2O_3) and ferromagnetic material (Fe).[13)]

4. Conclusion

We prepared a magneto-electric field effect transistor and investigated its magnetic and dielectric properties. The first tunnel layer of CeO_2 film has a highly oriented polycrystalline structure on a Si (111) substrate, while the gate insulator of the Cr_2O_3 film has preferentially 006-oriented structures. The sample showed ferromagnetic properties on a magnetization curve by the insertion of a MFG layer composed of Fe. The *C–V* curve shows hysteresis and a trace typical of a Si-MIS capacitor, indicating the carrier accumulation and depletion process in the interface between Si and the insulator. The hysteresis curve of a sample having a tunnel layer thickness of less than 10 nm has a clockwise carrier injection-type trace. The squareness of the hysteresis was enhanced by applying an external magnetic field of 0.5 T. These results indicate that this MIS capacitor contains a memorized floating gate, ME insulating layer, and ferromagnetic feature in one system.

References

1) N. Nur, S. Park, P. A. Sharma, J. S. Ahn, S. Guha and S.-W. Cheong, *Nature*, **429**, 392–395 (2004).
2) T. Lottermoser, T. Lonkai, U. Amann, D. Hohlwein, J. Ihringer and M. Fiebig, *Nature*, **430**, 541–544 (2004).
3) J. Wang, J. B. Neaton, H. Zheng, V. Nagarajan, S. B. Ogale, B. Liu, D. Viehland, V. Vaithyanathan, D. G. Schlom, U. V. Waghmare, N. A. Spaldin, K. M. Rabe, M. Wuttig and R. Ramesh, *Science*, **299**, 1719–1722 (2003).
4) Y. K. Yun, M. Noda and M. Okuyama, *Appl. Phys. Lett.*, **83**, 3981–3983 (2003).
5) S. Shtrikman and D. Treves, *Phys. Rev.*, **130**, 986–988 (1963).
6) E. Kita, A. Tasaki and K. Siratori, *Jpn. J. Appl, Phys.*, **18**, 1361–1366 (1979).
7) T. Yokota, T. Kuribayashi, M. Gomi, T. Shundo and Y. Sakakibara, *Advanced Materials Research*, **11–12**, 133–136 (2006).
8) M. Yoshimoto, H. Nagata, T. Tsukahara and H. Koinuma, *Jpn. J. Appl. Phys.*, **29**, L1199–L1202 (1990).
9) M. Yoshimoto, K. Shimozono, T. Maeda, T. Ohnishi, M. Kumagai, T. Chikyo, O. Ishiyama, M. shinohara and H. Koinuma, *Jpn. J. Appl. Phys.*, **34**, L688–L690 (1995).
10) A. K. Agyei and J. L. Birman, *J. Phys.:Condens. Matter*, **2**, 3007–3020 (1990).
11) P. H. Fang and W. S. Brower, *Phys. Rev.*, **129**, 1561 (1963).
12) S. M. Sze, "Semiconductor Physics, 2nd ed.," Wiley-Interscience, New York (1981) pp.496–500.
13) Ch. Binek, P. Borisov, X. Chen, A. Hochstrat, S. Sahoo and W. Kleemann, *Eur. Phys.*, J. B45, 197–201 (2005).